Journal of
Composites Science

MDPI

Article

Surface-Modified Wheat Straw for the Production of Cement-Free Geopolymer Composite: Effects of Wheat Variety and Pre-Treatment Method

Regina Kalpokaitė-Dičkuvienė *, Inna Pitak, Anastasiia Sholokhova, Rita Kriūkienė and Arūnas Baltušnikas

Laboratory of Materials Research and Testing, Lithuanian Energy Institute, Breslaujos St. 3, LT-44403 Kaunas, Lithuania; inna.pitak@lei.lt (I.P.); anastasiia.sholokhova@lei.lt (A.S.); rita.kriukiene@lei.lt (R.K.); arunas.baltusnikas@lei.lt (A.B.)

* Correspondence: regina.kalpokaite-dickuviene@lei.lt

Abstract: The development of new composite materials with specific properties and reduced environmental pollution can be achieved by the incorporation of agricultural residues, whose morphology is strongly affected by their variety and growing conditions. Herein, the functional properties of a cement-free geopolymer composite reinforced with straw from two wheat varieties (Ada and Malibu) were investigated through different straw pre-treatment methods and their surface modification with silane coupling agents. The characterization of the wheat surface and the geopolymer composites involved SEM-EDS, TGA, FTIR, and gas physisorption analysis methods supplemented with mechanical strength and moisture ingress measurements. Mild (23 °C) and severe (100 °C) physical pre-treatment methods with chemical soaking in 7.3 M isopropanol solution were applied on wheat straw. Tetraethoxysilane (TEOS) with octadecylamine was employed for chemical surface modification. The set of geopolymer compositions was prepared with untreated, pre-treated, and modified straws. The results revealed the hot pre-treatment method caused a higher degradation of siliceous layers of straw, especially in the Ada variety. The modification with TEOS resulted in irregular silane coating formation regardless of the wheat variety and pre-treatment method. Despite good interfacial bonding of the modified straw with the geopolymer matrix, the mechanical strength of the composites was reduced, although the resistance to water ingress slightly increased. Comparing both varieties, Ada wheat showed better performance than Malibu.

Keywords: wheat variety; straw; pre-treatment; modification; geopolymer; morphology

Citation: Kalpokaitė-Dičkuvienė, R.; Pitak, I.; Sholokhova, A.; Kriūkienė, R.; Baltušnikas, A. Surface-Modified Wheat Straw for the Production of Cement-Free Geopolymer Composite: Effects of Wheat Variety and Pre-Treatment Method. *J. Compos. Sci.* **2024**, *8*, 116. https://doi.org/10.3390/jcs8040116

Academic Editor: Salvatore Brischetto

Received: 28 February 2024
Revised: 14 March 2024
Accepted: 20 March 2024
Published: 22 March 2024

1. Introduction

High emissions of greenhouse gases and environmental pollution boost the development of sustainable composite materials. The huge generation of industrial by-products, municipal wastes, and agricultural residues is challenging in terms of their utilization and disposal. Therefore, their integration into composite materials appears to be environmentally viable. Geopolymers, among others, are receiving much attention due to their high potential to reduce carbon footprint [1,2]. Geopolymers are ceramic-like inorganic polymers produced at a temperature lower than 100 °C. They consist of chains of mineral molecules of aluminum hydroxyl and poly(siloxo) hexagonal linked with covalent bonds by creating a three-dimensional structure that provides high strength, durability, fireproofing, thermal insulation, etc. [2,3]. Various types of industrial waste materials, such as fly ash, slag, or kaolin sediments, may serve as a source of aluminosilicate material in geopolymer production and, therefore, provide a cement replacement, leading to a reduction in carbon dioxide emissions [4]. Incorporating agricultural residues into building materials has recently attracted more attention, resulting in the development of new composite materials with specific properties and reducing environmental pollution [5–11]. For the effective application

of biomass residues in composite materials, their surface pre-treatment is needed to remove components covering the surface of biomass, such as waxes, lignin, and hemicellulose, which reduce the compatibility or bonding strength with a matrix [8,12–15]. A survey of the literature shows that chemical or physicochemical pre-treatments utilizing organic solvents, molten oxalic dihydrate [13], sulphuric acid liquor [15], weak-base sodium carbonate solution [16], or hydrothermal pre-treatment coupled with an alkaline solution [17] are relatively fast and effective methods to disturb the structure and chemistry of lignin and cellulose. Biological enzyme technology and physical pre-treatment with steam by applying ultrasound or microwaves have also been investigated, enhancing the delignification efficiency important for bioenergy production [14,18]. Various methods, such as esterification, benzylation, acetylation, and organosolv or sol–gel coating techniques [19], have been used for the chemical modification of wheat straw involving chemical solutions, such as sodium hydroxide and sulphite, sulphuric acid, and hydrogen peroxide [20–22]. To increase the bonding strength between matrix and filler, the surface of the straw has been modified with various organic and non-organic materials. For example, the physical functionalization of wheat straw with graphene nanoparticles and attapulgite nano clay resulted in mechanical strengthening and water penetration reduction in modified alkali-activated materials [23]. The modification of wheat surfaces by covering them with flame retardants increased the thermal conductivity of cement-based composites [21]. Meanwhile, the application of silane coupling agents for wheat straw surface modification leads to the improvement in the water resistance and mechanical strength performance of polymeric composites [24,25]. Modifications with aminosilane, methacryl-functional silane, glycidoxypropyl-trimethoxysilane, and oxypropyl-trimethoxysilane are commonly used to increase the compatible interface between biomass and polymeric matrix [25]. Meanwhile, the application of tetraethyl orthosilicate (TEOS) for the deposition of silica-based coatings is rare [26,27]. The formation of a coating may occur through the addition of a hydrophobic precursor, such as methyltriethoxysilane, that interacts with the surface of the biomass [26]. The application of octadecylamine (ODA), which is an amine with a hydrophobic tail, may play a role in the stabilization of the silicon compounds and participate in condensation reactions forming a silica network on the surface of straw. The modification of the surface of wheat straw with TEOS and ODA has not been studied so far.

According to [28], soil characteristics and farming practices, such as wheat variety, sowing dates, and fertilization, combined with global warming effects, such as heat waves, drought, and water excess, alter the development of wheat plants and their morphology, physiology, and molecular responses. It suggests that the effects of wheat pre-treatment and modification methods may vary depending on the wheat variety and growing conditions. According to the literature survey, the common name of wheat, harvesting time, and reference to the supplier are provided in most studies, while more details on their variety or growing conditions are omitted. To the best of our knowledge, the impact of wheat variety on the functional properties of composite materials has not been studied so far.

Therefore, the effect of physical wheat pre-treatment methods and straw functionalization with a hydrophobic agent on the structural changes in the straw morphology of different varieties was investigated. Moreover, this study focused on creating a coating that improves the interfacial compatibility of wheat straw with the geopolymer matrix and investigated how the pre-treatment and chemical modification of the wheat straw surface of two varieties alter the functional properties of the geopolymer composite.

2. Materials and Methods

2.1. Raw Materials

2.1.1. Biomass Samples

Two types of wheat plants, Ada (A) and Malibu (M), were harvested in summer 2023 on an ecological farm in Dotnuva, Lithuania. Both varieties belong to different classes of wheat. More details on the wheat variety can be found elsewhere [29–31].

A wheat plant has four basic parts: the head with grains, stem, leaves, and roots. Stems contain nodes and internodes. Since the node's morphology significantly differs from the internode and does not undergo changes during thermal treatment [32,33], only the internodes of stems were selected for further experiments. Both wheat straw samples were chopped, their length was reduced to 2–5 mm, and then they were dried at 45 °C until they were of constant weight and sealed in plastic containers prior to further analysis.

2.1.2. Geopolymer Material

Metakaolin (MK) was selected as the source of aluminosilicate material, obtained after calcination of kaolin clay at 800 °C for 2 h. Kaolin clay's and MK's chemical composition and particle size are presented in detail elsewhere [34,35]. The activation solution was a sodium silicate solution (JSC Rameta, Vilnius, Lithuania), with a SiO_2/Na_2O ratio of 3.3 and a density of 1.25 g/cm^3. Pure (TG 99%) NaOH (Sigma Aldrich Merck, Darmstadt, Germany) was used to prepare a 12 M sodium hydroxide solution. Quartz sand with a particle size of 0.0–0.4 mm (JSC Anykščių kvarcas, Vilnius, Lithuania) was selected as the filler.

2.1.3. Chemical Treatment

Pure tetraethoxysilane (TEOS) (TG 99%) with a molecular weight (MW) of 208.33 g/mol, octadecylamine (TG 90%) with an MW of 269.51 g/mol, ethanol (TG 99.8%) with an MW 46.07 g/mol, and isopropanol (TG 70%) with an MW of 60.1 g/mol were purchased from Sigma Aldrich.

2.2. Wheat Pre-Treatment and Modification Procedure

The whole pre-treatment and modification procedure and the sequence are presented in Figure 1. At first, the chopped wheat straw was placed in the flasks with distilled water and stirred in a magnetic stirrer for 10 min; then, the water was renewed and the washing procedure was repeated. After that, samples were dried in an oven and denoted as A and M (Table 1). Then, a set of samples was boiled in water for 2 h. Boiled and non-boiled (hot and cold treatment, respectively) samples were immersed in an isopropanol solution (chemical treatment). The molarity of the isopropanol solution, obtained after isopropanol dilution with water (50/50), was 7.3 M. After 40 h of soaking, the samples were used for the modification procedure when the chemical reaction between wheat straw and the modifying agent was initiated (Figure 1, Table 1). After modification, samples were filtrated, washed with water and ethanol, and oven-dried at 70 °C for 24 h.

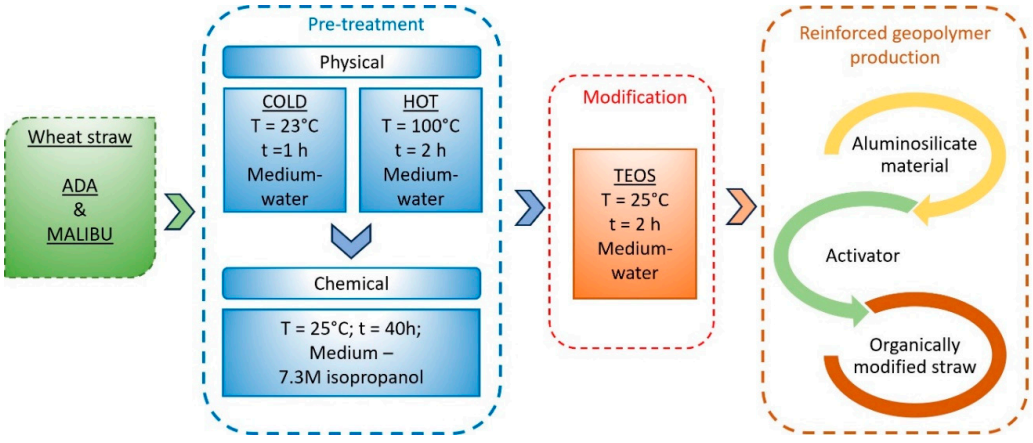

Figure 1. Schematic diagram of wheat straw pre-treatment and modification steps.

Table 1. Nomenclature of samples and their pre-treatment (A—Ada; M—Malibu; C—cold; H—hot; T—modification with TEOS).

Sample ID	Symbols/ Color	Physical Pre-Treatment	Chemical Pre-Treatment	Modification
A//M	□//Δ	Washed in water and dried	-	-
AC//MC	□//Δ	Washed in water 1 h	Chemical pre-treatment in 7.3 M isopropanol solution	-
AH//MH	□//Δ	Boiled in water 2 h	Chemical pre-treatment in 7.3 M isopropanol solution	-
AC-T//MC-T	■//▲	Washed in water 1 h	Chemical pre-treatment in 7.3 M isopropanol solution	Modification with TEOS
AH-T//MH-T	■//▲	Boiled in water 2 h	Chemical pre-treatment in 7.3 M isopropanol solution	Modification with TEOS

2.3. Geopolymer Samples' Production and Testing

M. Chougan et al. [23] demonstrated that the incorporation of 1% of wheat straw gives moderate mechanical strength to geopolymer compositions; therefore, in this study, we used the same dosage of straw to evaluate the impact of wheat straw variety, pre-treatment, and modification on the functional properties of the geopolymer. Mix composition was kept the same for all samples. First, NaOH (7 wt%) was mixed with Na_2SiO_3 (38 wt%) and water. The solution was cooled and cured for 24 h until use. Then, MK (41 wt%) and sand (ratio 1:3) were mixed until a homogeneous paste was obtained. Finally, the straw was added to the paste. A water-to-solid ratio of 0.6 was selected to avoid the incorporation of plasticizer. The nomenclature of geopolymers was the same as in Table 1 with the letter "G" in front (for example, A—ADA wheat straw; GA—geopolymer with ADA straw).

After mix preparation, pastes were poured into four prismatic and six cubic molds and left to cure at 23 ± 2 °C and RH 90% for 24 h. Demolded samples were cured at the same conditions for 56 days to ensure gel formation, polycondensation, nucleation, and solidification reactions took place. To avoid uncertainties due to unfinished geopolymerization, all samples were heated at 80 °C for 24 h before the mechanical tests. Compressive and flexural strength tests were performed based on EN 196-1 standard using the Zwick Roell universal testing machine and 1 mm/min load rate. The water absorption test was performed in accordance with standard ASTM C642 on cubic samples, while broken prismatic samples were used for the capillary imbibition test under the procedure described in [34,36]. Based on these measurements, the volume of permeable pore space (VPP), water absorption (WA), and cumulative water absorption rate for each sample were calculated.

2.4. Characterization

Raw, pre-treated, and modified wheat straws were analyzed by TGA, FTIR, gas (N2) physisorption, and SEM-EDS methods.

Thermal degradation of wheat straw was examined by thermalgravimetric analysis (TGA). A nearly 20 mg straw sample was placed in a LINSEIS STA PT1600 thermal analyzer and heated up to 700 °C under airflow at a heating rate of 10 K/min.

The FTIR spectra were obtained with a Bruker Alpha FTIR Spectrometer as the average of 32 scans in the wavenumber range of 4000–400 cm^{-1} with a resolution of 4 cm^{-1}. Three spectra were obtained for each sample, the background was removed, and then the average of these three spectra was created and used for further analysis.

The nitrogen physical adsorption technique [37] was used to determine the specific surface area based on the BET method, total pore volume, and average pore diameter. The measurements were performed on a Quantachrome Autosorb iQ analyzer in a p/p_0 range up to 0.99.

The morphology analysis of wheat straw was performed on a Zeiss EVO MA SEM instrument at an accelerating voltage of 5 kV. Before imaging, samples were dried in a

vacuum and gold-coated in an SPI sputter coater. Geopolymer samples were analyzed at an accelerating voltage of 20 kV. An energy-dispersive X-ray detector system (EDS) from Bruker AXS XFlash 6/10 was used for elemental composition analysis of the samples.

3. Results

3.1. Characterization of Wheat Straw

Figure 2 shows the outer surface and cross-section of the untreated straw samples of both varieties. As can be seen, the surfaces are covered with hydrophobic cuticula, containing siliceous layers, which regulate water balance and protect in the plant [38]. The cross-sectional views are the same for both varieties and consist of vascular bundles and parenchyma in the middle and epidermis cells on the outer surface of the straw.

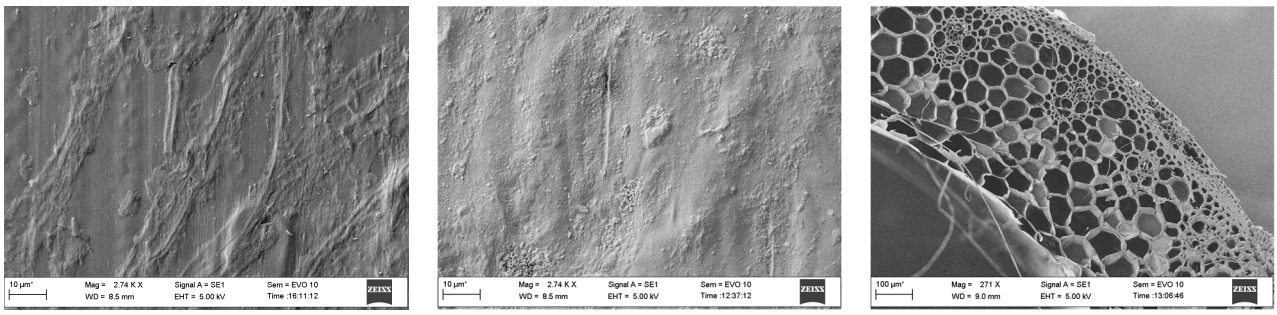

(**a**) (**b**) (**c**)

Figure 2. SEM images of untreated wheat straw: (**a**) outer surface of A sample; (**b**) outer surface of M sample; (**c**) cross-section of straw. In (**a**,**b**), the scale bar is 10 µm, magnification—2740 times; a scale of 100 µm with a magnification of 271 is used in (**c**).

Cold pre-treatment affected the cuticula and siliceous layers without significant membrane damage through the formation of pinholes due to the removal of fatty acids (Figure 3a,c). (Images were taken in backscattering mode to see the distribution of silicon.)

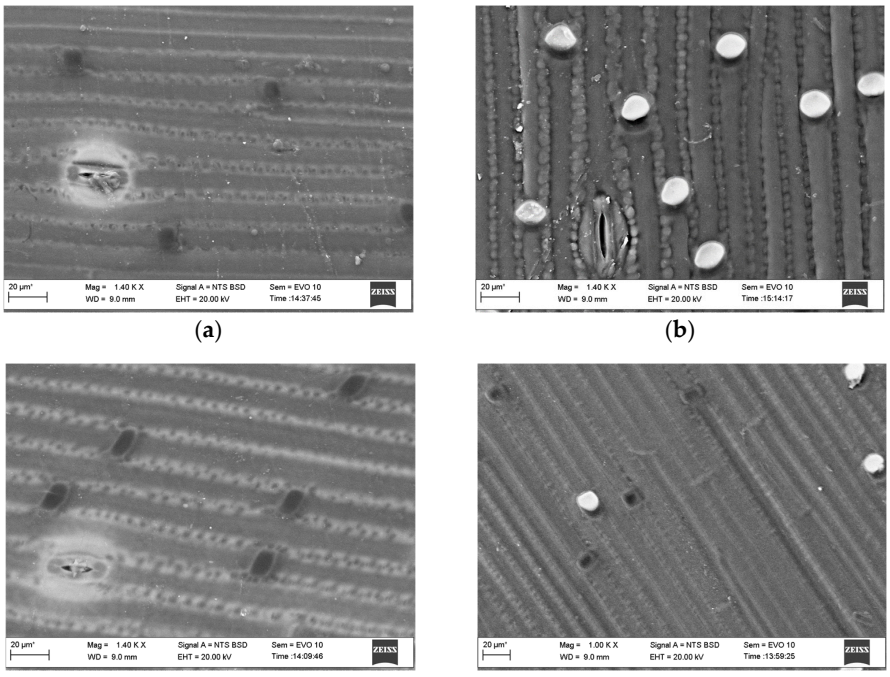

(**a**) (**b**)

(**c**) (**d**)

Figure 3. SEM images of pre-treated wheat straw: (**a**,**b**) outer surface of AC and AH samples; (**c**,**d**) outer surface of MC and MH. The scale bar is 20 µm; magnification—1400 times.

The more obvious decomposition of fibers in the vascular bundle and parenchyma leading to the exfoliation of cuticula and siliceous layers [39] occurred after the hot treatment (Figure 3b,d). It seems that the degradation of fibers was greater in the A sample than in M (Figure 3), where more pinholes formed due to the removal of silicon-containing particles. A similar morphology of the outer surface of wheat was observed by others after neutral lipase and cellulase treatment [39], where the degradation of the vascular bundle was explained by the reduction in bonding forces between the keratinous and siliceous layers. SEM-EDS elemental analysis confirmed a decline in silicon content on the surface of both types of straw, which was substantially reduced after the hot pre-treatment method (Table 2).

Table 2. Effect of pre-treatment on the elemental composition of wheat straw surface.

Sample ID	Si, at % (StD)	O/C Ratio
A	6.77 (3.4)	0.86
M	5.01 (2.5)	0.74
AC	2.98 (1.0)	0.81
MC	2.45 (1.8)	0.79
AH	<1.0 (0.4)	0.68
MH	<1.0 (0.4)	0.61
AC-T//AH-T	11.8 (2.2)	2.09
MC-T//MH-T	12.1 (1.8)	2.10

The degradation of straw was monitored by thermogravimetric analysis. Figure 4 shows the TG and DTG profiles. In the oxidizing atmosphere, the degradation reactions of the main constituents of straw, such as hemicellulose, cellulose, and lignin, take place [24,25,40]. At around 130 °C during the dehydration and desorption stage [40], the evaporation of moisture and degradation of hemicellulose occurs. The burnout of hemicellulose and cellulose with the removal of volatile matter starts from 200 °C, while the main decomposition of hemicellulose and cellulose lasts up to 370 °C in the combustion stage (Figure 4). During the char combustion stage, over 370 °C [40], mainly the lignin decomposes. It is worth mentioning that the decomposition of lignin starts in the same temperature range as that of hemicellulose and cellulose, but the process duration and chemical reactions depend on the heating rate and degradation atmosphere [41]. Figure 4 shows that the TGs of all samples have a similar shape, but two coldpre-treated and modified samples (AC-T and MC-T) distinguish, especially over 370 °C. It suggests that the effectiveness of modification depends both on the pre-treatment method and the variety of wheat, which is in line with the SEM observations (Figure 3). Weight losses, summarized in Table 3, show that the dehydration and degradation of hemicellulose (25–200 °C) proceed faster in the A sample than in M; meanwhile, the degradation of cellulose with lignin (200–370 °C) depends more on the pre-treatment method than on the wheat variety.

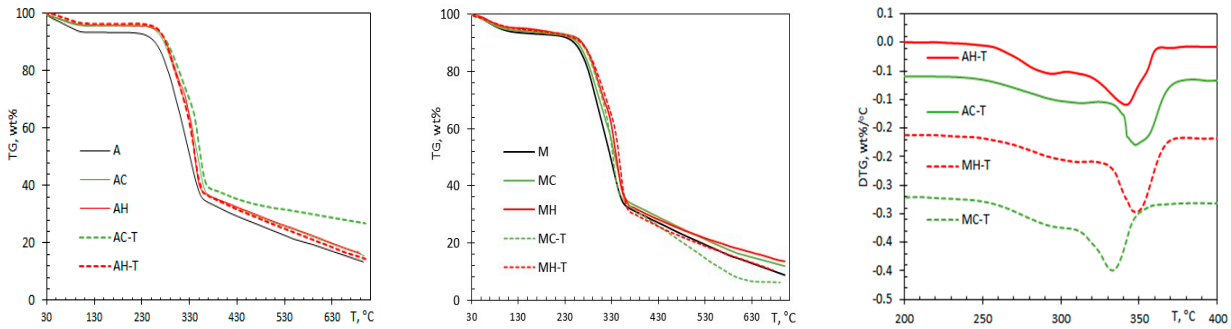

(**a**) (**b**) (**c**)

Figure 4. TG curves of untreated, pre-treated, and modified wheat straw: (**a**) ADA variety; (**b**) MALIBU variety; (**c**) DTG curves of modified wheat straws.

Table 3. Summary of TGA data.

Sample ID	Relative Mass Change Δm (%)		
	25–200 °C	**200–370 °C**	**370–700 °C**
A//M	6.4//6.6	59.4//61.0	20.7//22.9
AC//MC	4.3//5.9	59.9//60.9	20.5//21.3
AH//MH	4.1//4.9	58.9//62.7	21.1//18.8
AC-T//MC-T	4.0//5.7	57.6//60.1	11.6//27.2
AH-T//MH-T	4.6//4.5	60.0//64.5	21.9//21.0

The DTG curves in the cellulose decomposition range are presented in Figure 4c. The shift in the peak to the higher temperature indicates an increased thermal stability of straws attributed to the greater removal of hemicellulose, cellulose, and lignin together with the formation of a protective layer preventing the destruction of straw components [24,25,41].

The SEM and TG observations correlate well with the nitrogen porosimetry results that provide valuable insights into the structural changes the straw samples undergo under different treatment conditions. The data obtained by the N_2 physisorption, such as the total pore volume, specific surface area (BET), and average pore diameter, are summarized in Figure 5. Due to fragmentation, the degradation of straw constituents, and the formation of pinholes, the total pore volume tends to increase; however, the M samples show nearly twice higher values than the A samples after both cold and hot pre-treatment. This is in line with observations presented in [14], where an increase in the temperature of the pre-treatment medium (both water and an acidic solution) by 15 °C (from 35 °C up to 50 °C) resulted in a doubling of the total pore volume and BET of straw. In this study, the threefold higher BET area of the A samples indicates that the hot treatment increases the surface roughness, which, according to [41], may occur due to the possible formation of lignin scraps. The higher weight loss over 370 °C for the AH sample confirms this assumption (Table 3). On the contrary, the reduction in BET in the M samples suggests greater removal of substances from the surface.

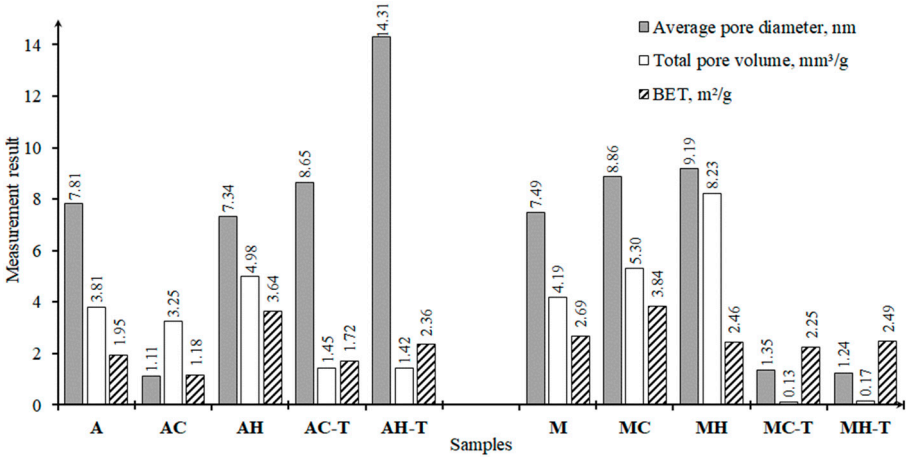

Figure 5. The summary of nitrogen adsorption measurements results for wheat plants ADA (A) and MALIBU (M).

The images of the wheat straw surfaces modified with TEOS together with the elemental distribution of silicon and carbon are presented in Figure 6. It can be seen that modification formed an irregular layer on the surface of the straw irrespective of wheat variety. However, a nearly constant BET value of the modified M samples and an increase in BET for the A samples indicate that the modification effectiveness depends on the pre-treatment method. Moreover, a substantial reduction in total pore volume suggests a larger part of the surface is covered by the modifying agent (Figure 6). The reason for this irregular layer formation may lie in the insufficient removal of straw components, which is visible

as a shoulder peak around 300 °C (Figure 4c), as well as the concentration of modifying agents [24]. The impact of concentration was out of the scope of this study, though it will be considered in future research. However, a doubling of Si content and an increase in the O/C ratio (Table 2) indicate the presence of active chemical groups on the surface of the straw, which was further confirmed by FTIR.

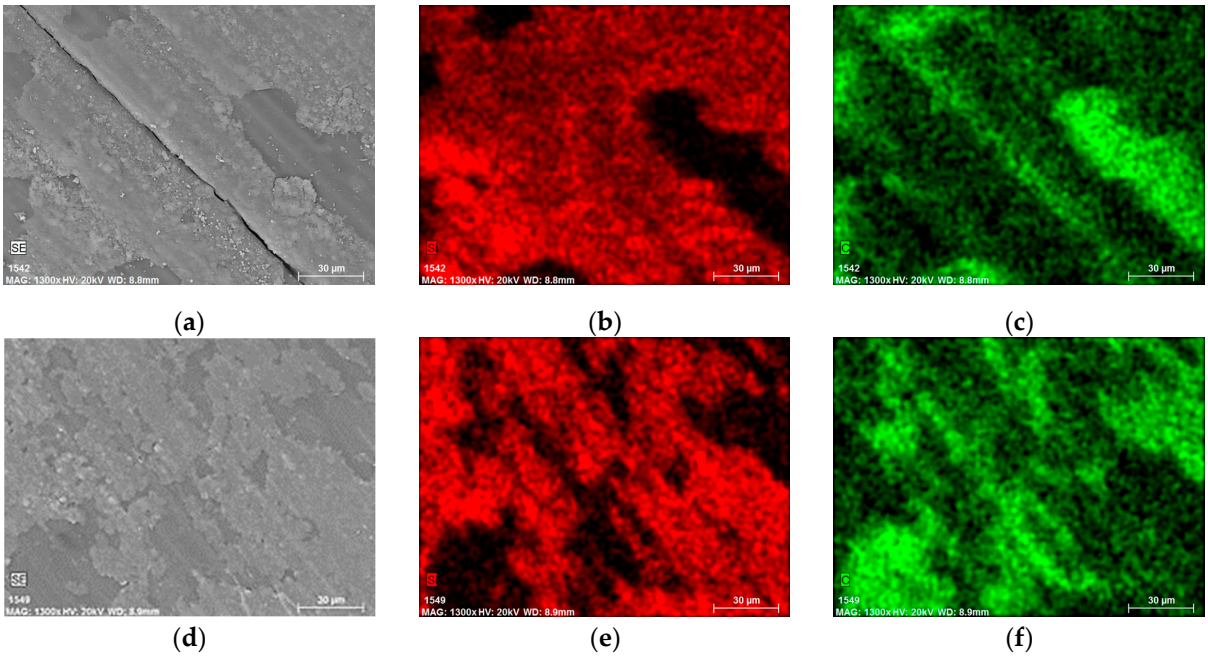

Figure 6. Mapping of pre-treated and modified wheat straw: SEM image of AC-T (**a**) with silicon (**b**) and carbon elemental distribution (**c**); SEM image of MH-T (**d**) with silicon (**e**) and carbon elemental distribution (**f**). The scale bar is 30 µm; magnification—1300 times.

The FTIR spectra presented in Figure 7 show the absorption peaks at approximately 2850 and 2920 cm^{-1}, which are usually associated with the antisymmetric stretching vibration of C–H in the saturated aliphatic CH2 groups of lignin [16,42]. A reduction in the intensity of these bands indicates that the cold and hot pre-treatments decreased the aliphatic CH2 groups in lignin. Notably, this decrease was more pronounced in the "A" samples compared to the "M".

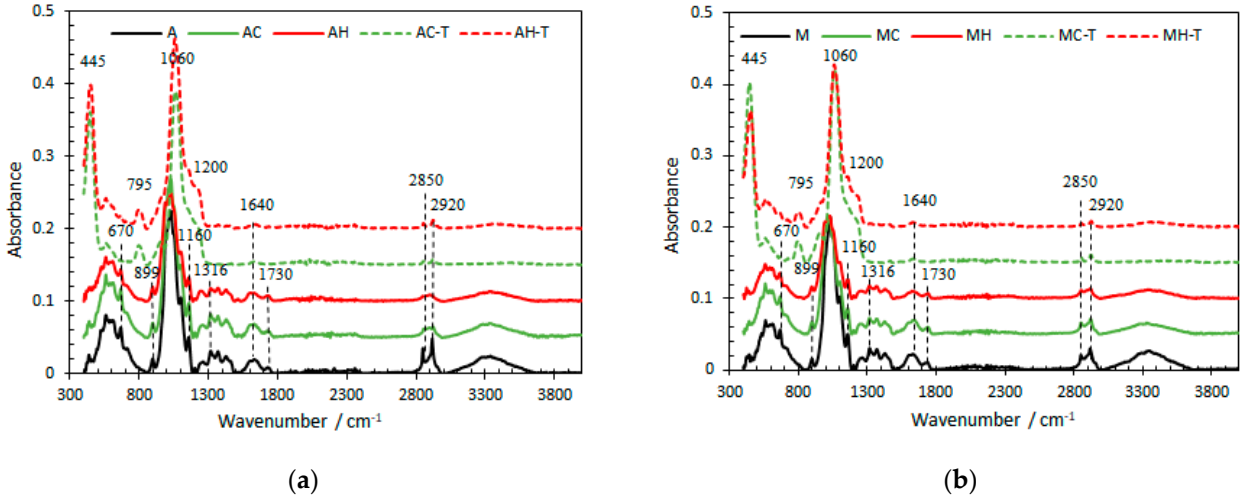

Figure 7. FTIR spectra of untreated, pre-treated, and modified wheat straw: (**a**) ADA wheat straw; (**b**) MALIBU wheat straw.

The carboxyl stretching band at 1730 cm^{-1} [43], characteristic of carboxylic acid groups in hemicellulose, exhibited no observable change in both wheat varieties. The absorption peak in the region near 1640 cm^{-1}, corresponding to the stretching vibrations of C=O bonds, is indicative of lignin content [16]. In the case of cold pre-treatment, there was minimal impact on this band, suggesting a limited effect on lignin. However, in the hot pre-treatment case, a slight reduction in this absorption peak was observed, indicating a potential degradation or alteration in the lignin structure. Another indicator of lignin degradation is the decrease in the peak at 1315 cm^{-1}, corresponding to the C–O vibrations of the syringyl ring [16]. In the M samples, both the cold and hot pre-treatments led to a reduction in peak intensity. Conversely, in the "A" samples, cold pre-treatment showed no effect on this peak, while hot pre-treatment resulted in a reduction, highlighting variations in the impact of different pre-treatments on lignin components in the two sample types. The band at 1160 cm^{-1} is associated with the antisymmetric stretching of C–O–C glycosidic linkages in both cellulose and hemicellulose [42]. Both pre-treatments led to a reduction in this peak, with hot treatment being more effective. When comparing the two wheat straw varieties, the M samples exhibited a higher reduction, indicating a greater impact of the pre-treatments on the glycosidic linkages. No observable change was noted in the absorption peak associated with ß-glycoside linkages in lignin and cellulose at 899 cm^{-1} [44]. The band at 670 cm^{-1}, characteristic of cellulose and representing an OH torsional vibration band [42], remained unaffected by cold pre-treatment. However, hot pre-treatment resulted in a slight reduction in this band.

The spectra of the modified wheat straw surface (MC-T; MH-T//AC-T; AH-T) revealed prominent peaks at approximately 1200, 1060, 795, and 445 cm^{-1} (Figure 7). Peaks near 1060 cm^{-1} and 445 cm^{-1} are attributed to Si–O stretching, indicating the presence of silicon–oxygen bonds [16,45]. The peak at 1200 and 795 cm^{-1} is attributed to the symmetrical stretching vibrations of the Si–O–Si band [46,47]. The reduced intensity of the peak at 3417 cm^{-1} suggests the consumption of O-H during modification reactions [24]. All these intensities indicate the formation of a siloxane network on the wheat straw surface.

3.2. Characterization of Geopolymers with Wheat Straw

Water ingress curves of geopolymers with pre-treated and modified straws are presented in Figure 8.

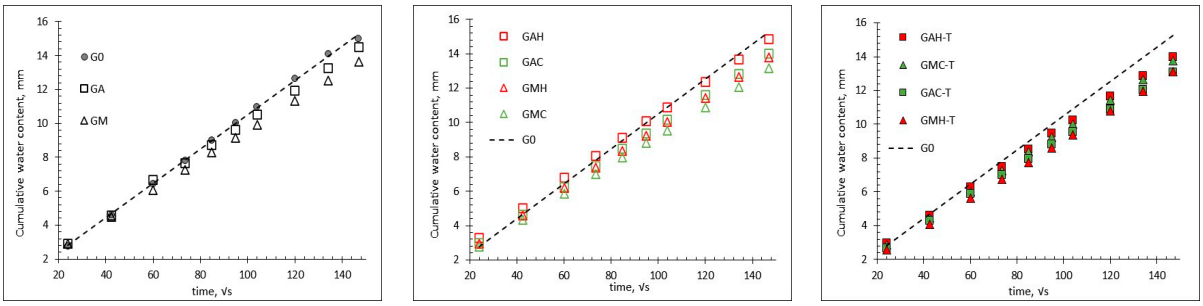

(**a**) (**b**) (**c**)

Figure 8. Cumulative water content of geopolymers: (**a**) geopolymers without straw (G0) and with unmodified straw of different varieties (GA, GM); (**b**) geopolymers with physically treated straw; (**c**) geopolymers with modified straw. See the nomenclature in Table 1.

Water sorption increases gradually over time for all compositions, though the suction rate is slightly slower in the compositions with modified straw, which could be interpreted as being due to the formation of a protective, but non-uniform, silane layer on the surface (Figure 6). On the other hand, the pre-treatment method has less effect on the water ingress rate than the wheat straw variety, where the M straw showed the best results among all samples. According to [24], the modification with silane causes an improvement in

interfacial adhesion, increasing the overall water resistance and mechanical strength of the composite. However, the mechanical strength and total water absorption data, presented in Figure 9, showed opposite results. In general, adding 1% of straw to the geopolymer composition resulted in a reduction in flexural and compressive strength, although the application of the A straw variety gave better results than M (Figure 9). Compared to the reference sample, the compressive strength reduction did not exceed 10% in all sets with straw. On the contrary, the impact of wheat variety was more significant on flexural strength, which reduced for 11–27% in samples with the A straw, while a 15–30% lower strength was shown by the samples with M. The impact of the straw pre-treatment method is also visible. The incorporation of cold pre-treated straws lowered compressive strength to less than 3%, whereas a three times greater reduction is seen for the hot-pre-treated samples, where the maximum (−12%) is found for the GMH—Δ—sample. On the contrary, the chemical modification of straw, especially hot-treated, results in an enhancement in flexural strength indicating improved interconnected polymerization and adhesion between the straw and matrix [23,24]. These data correlate well with the water ingress rate results (Figure 8c), which suggest the lowered connectivity of capillary pores. However, the distribution of permeable voids (Figure 9b) implies the formation of a more porous geopolymer structure causing the reduced resistance to compressive loads (Figure 9a).

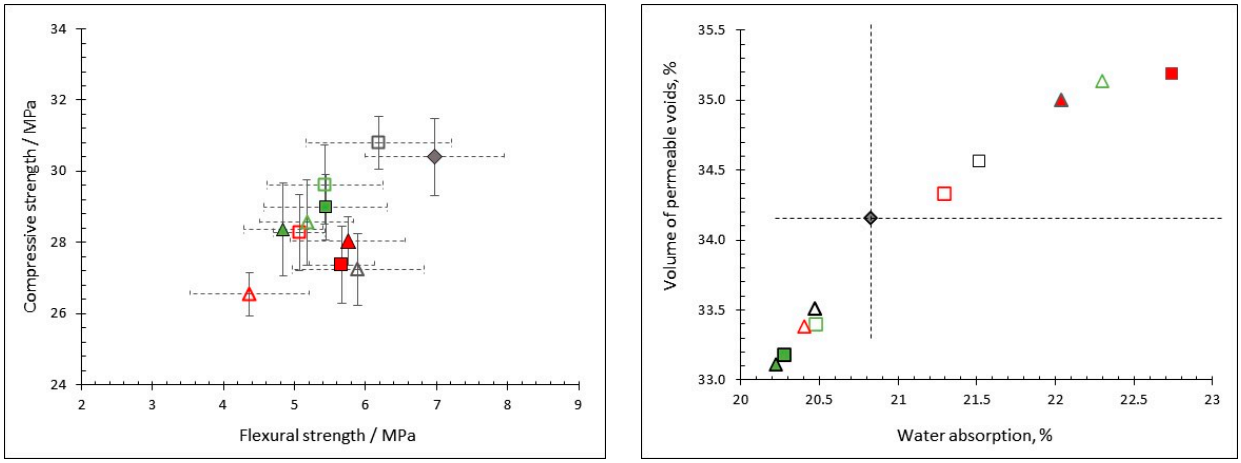

Figure 9. Mechanical strength (**a**) and water adsorption (**b**) of geopolymers reinforced with various treated wheat straws. Filled diamond (♦) corresponds to the reference material (G0). See the nomenclature in Table 1.

4. Discussion

For wheat straw modification, two chemical compounds with different properties were used to initiate the silanization process, involving the covalent attachment of silane compounds on the surface of straw [25]. Since TEOS undergoes condensation reactions, a siloxane network (Si-O-Si) was formed on the straw surface (Figure 6). The amine group in the octadecylamine may form hydrogen bonds with the polar hydroxyl groups of wheat, such as cellulose, hemicellulose, and lignin [24,25], by introducing hydrophobic alkyl chains on the surface of straw. Therefore, the surface of straw, which itself has hydrophilic hydroxyl groups, may become more resistant to water. The reduced intensity at 1640 cm^{-1} characterizing the water absorbance of wheat [8,25] confirms this assumption (Figure 7), explaining the improved geopolymer composite's water resistance (Figure 8). However, the volume of permeable voids and mechanical strength significantly differ between the compositions with the modified straw after cold and hot pre-treatment methods, suggesting changes at the microstructural level.

The morphology observation of geopolymer composites, presented in Figure 10, revealed fairly good interfacial adhesion between the silane-modified straw and matrix,

which contradicts other studies [4,14,24,25] where the size of the straw was nearly ten times smaller than that used in this study. Figure 10 shows that, despite the good adhesion, the surface of the straw is full of cracks which are also visible on the bottom of the bedding place of the straw, from which the straw was removed during sample preparation. The relief of the bottom reiterates the surface of TEOS-modified straw (Figure 6). Moreover, a line scan shows a nearly equal distribution of Al, Si, and Na on the surface of the straw with the absence of carbon (the main component of straw), confirming the chemical interaction between the modified straw and the matrix. Furthermore, the damaged structure of the modified straw was observed in the geopolymer composites regardless of the wheat pre-treatment method or variety. It seems that the strength of the modified straw, more than interfacial bonding or the irregularity of silane coating, is a sensitive factor reducing the strength of the geopolymer matrix and forming additional gaps for the penetration of water. The results of this study and the observations made by others [23,24] infer that surface-functionalizing agents on pre-treated straw may lead to an enhancement in the functional properties of geopolymer composites if the particle size of the straw is considered. Aside from the influence of particle size, the loading content and the optimal dosage of the silane coupling agent should be investigated to create composites with new potential applications.

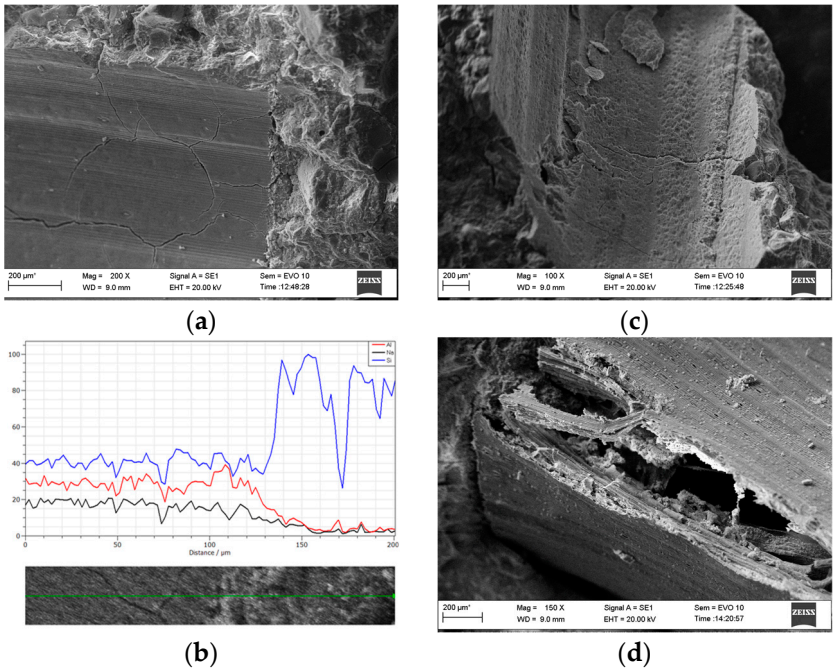

Figure 10. Geopolymer with the modified straw: (**a**) adhesion between geopolymer matrix and straw; (**b**) line scan on the boundary; (**c**) the bedding place of straw; (**d**) the damaged structure of the modified straw in the geopolymer. The scale bar is 200 µm; magnification—100–200 times.

5. Conclusions

Cement-free geopolymers reinforced with wheat straw were developed by investigating the effect of straw variety, surface pre-treatment methods, and surface modification with a silane coupling agent on the functional properties of composites. SEM and FTIR characterization revealed that the hot-pre-treatment method resulted in a greater removal of waxes, degradation of siliceous layers, and formation of pinholes on the surface of wheat than cold pre-treatment; meanwhile, the effect of wheat variety was less evident. Regardless of the wheat variety, the modification of the straw surface with TEOS was more effective after hot treatment even though the deposition was irregular. The mechanical performance of geopolymers reinforced with treated, untreated, and modified straws was reduced to a different extent, though compositions with the Ada variety showed better results than those with Malibu. Compared to the reference sample, the compressive strength reduc-

tion did not exceed 10% in all sets with straw. Meanwhile the flexural strength reduced from 10 to 30%, where better performance was shown by the chemically modified straw. The results revealed that the alterations in wheat straw itself diminish the performance of geopolymers; however, the surface modification of M straw with the silane coupling agent boosted the water resistance of the composites, reducing the sorptivity by more than 15%.

These findings contribute to a better understanding of how different wheat varieties and their pre-treatments influence the properties of straw-based materials, with implications for various applications in agriculture, construction, and environmental remediation.

Author Contributions: Conceptualization and methodology, R.K.-D. and A.B.; investigation and validation, R.K.-D., I.P., A.S. and A.B.; formal analysis, R.K.; writing—original draft preparation, R.K.-D., I.P., A.S. and A.B.; writing—review and editing, project administration, and funding acquisition, R.K.-D. All authors have read and agreed to the published version of the manuscript.

Funding: This work was carried out in the framework of the interinstitutional RTO Lithuania research program.

Data Availability Statement: Data will be available on the request.

Acknowledgments: The authors would like to acknowledge the RTO project "KarboIzotopas" partners from LAMMC for providing the samples. Authors extend their gratitude to Irena Lukošiūtė for her support and fruitful discussions.

Conflicts of Interest: The authors declare no conflicts of interest. The funders had no role in the design of the study; in the collection, analyses, or interpretation of data; in the writing of the manuscript; or in the decision to publish the results.

References

1. Farhan, K.Z.; Johari, M.A.M.; Demirboğa, R. Assessment of important parameters involved in the synthesis of geopolymer composites: A review. *Constr. Build. Mater.* **2020**, *264*, 120276. [CrossRef]
2. Sambucci, M.; Sibai, A.; Valente, M. Recent Advances in Geopolymer Technology. A Potential Eco-Friendly Solution in the Construction Materials Industry: A Review. *J. Compos. Sci.* **2021**, *5*, 109. [CrossRef]
3. Walkley, B. Geopolymers. In *Encyclopedia of Engineering Geology*; Springer: Cham, Switzerland, 2018; pp. 1–2. [CrossRef]
4. da Silva Alves, L.C.; dos Reis Ferreira, R.A.; Bellini Machado, L.; de Castro Motta, L.A. Optimization of metakaolin-based geopolymer reinforced with sisal fibers using response surface methology. *Ind. Crops Prod.* **2019**, *139*, 111551. [CrossRef]
5. Walbrück, K.; Drewler, L.; Witzleben, S.; Stephan, D. Factors influencing thermal conductivity and compressive strength of natural fiber-reinforced geopolymer foams. *Open Ceram.* **2021**, *5*, 100065. [CrossRef]
6. Koh, C.H.; Kraniotis, D. A review of material properties and performance of straw bale as building material. *Constr. Build. Mater.* **2020**, *259*, 120385. [CrossRef]
7. Koh, C.; Gauvin, F.; Schollbach, K.; Brouwers, H. Upcycling wheat and barley straws into sustainable thermal insulation: Assessment and treatment for durability. *Resour. Conserv. Recycl.* **2023**, *198*, 107161. [CrossRef]
8. Fan, Q.; Han, G.; Cheng, W.; Tian, H.; Wang, D.; Xuan, L. Effect of intercalation structure of organo-modified montmorillonite/polylactic acid on wheat straw fiber/polylactic acid composites. *Polymers* **2018**, *10*, 896. [CrossRef] [PubMed]
9. Jiang, D.; Lv, S.; Jiang, D.; Xu, H.; Kang, H.; Song, X.; He, S. Effect of modification methods on water absorption and strength of wheat straw fiber and its cement-based composites. *J. Build. Eng.* **2023**, *71*, 106466. [CrossRef]
10. Zou, S.; Li, H.; Liu, L.; Wang, S.; Zhang, X.; Zhang, G. Experimental study on fire resistance improvement of wheat straw composite insulation materials for buildings. *J. Build. Eng.* **2021**, *43*, 103172. [CrossRef]
11. Yilma, W.M.; Singh, B.; Asrat, G.; Hossain, N. Taguchi Method Optimization of Water Absorption Behavior by Wheat Straw-Basalt Hybrid Brake Pad Composite. *J. Compos. Sci.* **2023**, *7*, 62. [CrossRef]
12. Ghaffar, S.H.; Fan, M. An aggregated understanding of physicochemical properties and surface functionalities of wheat straw node and internode. *Ind. Crops Prod.* **2017**, *95*, 207–215. [CrossRef]
13. Jiang, J.; Fu, J.; An, N.; Zhang, Y.; Chen, X.; Wang, L. Rapid and effective molten oxalic acid dihydrate pretreatment to enhance enzymatic saccharification for biohydrogen production by efficient coextraction of lignin and hemicellulose in wheat straw. *Chem. Eng. J.* **2023**, *475*, 146422. [CrossRef]
14. Gaudino, E.C.; Grillo, G.; Tabasso, S.; Stevanato, L.; Cravotto, G.; Marjamaa, K.; Pihlajaniemi, V.; Koivula, A.; Aro, N.; Uusitalo, J.; et al. Optimization of ultrasound pretreatment and enzymatic hydrolysis of wheat straw: From lab to semi-industrial scale. *J. Clean. Prod.* **2022**, *380*, 134897. [CrossRef]
15. Fougere, D.; Nanda, S.; Clarke, K.; Kozinski, J.A.; Li, K. Effect of acidic pretreatment on the chemistry and distribution of lignin in aspen wood and wheat straw substrates. *Biomass Bioenergy* **2016**, *91*, 56–68. [CrossRef]

16. Deng, Y.; Qiu, Y.; Yao, Y.; Ayiania, M.; Davaritouchaee, M. Weak-base pretreatment to increase biomethane production from wheat straw. *Environ. Sci. Pollut. Res.* **2020**, *27*, 37989–38003. [CrossRef] [PubMed]
17. Pan, N.; Jiang, B.; Hu, J.; Huang, M.; He, J.; Jiang, Q.; Zhao, L.; Shen, F.; Tian, D. The coupling effects between acid-catalyzed hydrothermal pretreatment and acidic/alkaline deep eutectic solvent extraction for wheat straw fractionation. *Bioresour. Technol.* **2023**, *386*, 129579. [CrossRef] [PubMed]
18. Chougan, M.; Ghaffar, S.H.; Al-Kheetan, M.J.; Gecevicius, M. Wheat straw pre-treatments using eco-friendly strategies for enhancing the tensile properties of bio-based polylactic acid composites. *Ind. Crops Prod.* **2020**, *155*, 112836. [CrossRef]
19. Sharifi, A.; Mousavi, S.R.; Ghanemi, R.; Mohtaramzadeh, Z.; Asheghi, R.; Mohammadi-Roshandeh, J.; Khonakdar, H.A.; Hemmati, F. Extruded biocomposite films based on poly(lactic acid)/chemically-modified agricultural waste: Tailoring interface to enhance performance. *Int. J. Biol. Macromol.* **2023**, *233*, 123517. [CrossRef]
20. JTong, J.; Wang, X.; Kuai, B.; Gao, J.; Zhang, Y.; Huang, Z.; Cai, L. Development of transparent composites using wheat straw fibers for light-transmitting building applications. *Ind. Crops Prod.* **2021**, *170*, 113685. [CrossRef]
21. Jiang, D.; Jiang, D.; Lv, S.; Cui, S.; Sun, S.; Song, X.; He, S.; Zhang, J. Effect of modified wheat straw fiber on properties of fiber cement-based composites at high temperatures. *J. Mater. Res. Technol.* **2021**, *14*, 2039–2060. [CrossRef]
22. Jiang, D.; An, P.; Cui, S.; Xu, F.; Tuo, T.; Zhang, J.; Jiang, H. Effect of leaf fiber modification methods on mechanical and heat-insulating properties of leaf fiber cement-based composite materials. *J. Build. Eng.* **2018**, *19*, 573–583. [CrossRef]
23. Chougan, M.; Ghaffar, S.H.; Sikora, P.; Mijowska, E.; Kukułka, W.; Stephan, D. Boosting Portland cement-free composite performance via alkali-activation and reinforcement with pre-treated functionalised wheat straw. *Ind. Crops Prod.* **2022**, *178*, 114648. [CrossRef]
24. Song, W.; Yang, Z.; Zhang, S.; Fei, B.; Zhao, R. Properties enhancement of poly(β-hydroxybutyrate) biocomposites by incorporating surface-modified wheat straw flour: Effect of pretreatment methods. *Int. J. Biol. Macromol.* **2023**, *232*, 123456. [CrossRef] [PubMed]
25. Chen, K.; Li, P.; Li, X.; Liao, C.; Li, X.; Zuo, Y. Effect of silane coupling agent on compatibility interface and properties of wheat straw/polylactic acid composites. *Int. J. Biol. Macromol.* **2021**, *182*, 2108–2116. [CrossRef] [PubMed]
26. Hussain, A.; Calabria-Holley, J.; Jiang, Y.; Lawrence, M. Modification of hemp shiv properties using water-repellent sol–gel coatings. *J. Sol-Gel Sci. Technol.* **2018**, *86*, 187–197. [CrossRef] [PubMed]
27. Wang, H.; Zhen, Z.; Yao, S.; Li, S. Synthesis of high acid-resistant ultramarine blue pigment through coal gangue, industrial zeolite waste and corn straw waste recycling. *Resour. Chem. Mater.* **2022**, *1*, 137–145. [CrossRef]
28. Le Gouis, J.; Oury, F.-X.; Charmet, G. How changes in climate and agricultural practices influenced wheat production in Western Europe. *J. Cereal Sci.* **2020**, *93*, 102960. [CrossRef]
29. Toleikiene, M.; Zvirdauskiene, R.; Suproniene, S.; Arlauskiene, A.; Brophy, C.; Kadziuliene, Z. Soil microbial functional diversity responds to plant-based organic fertlisers depending on the group of carbon sources. *Pol. J. Environ. Stud.* **2021**, *30*, 2755–2768. [CrossRef]
30. Toleikienė, M.; Arlauskienė, A.; Šarūnaitė, L.; Šidlauskaitė, G.; Kadžiulienė, Ž. The effect of plant-based organic fertilisers on the yield and nitrogen utilization of spring cereals in the organic cropping system. *Zemdirbyste* **2020**, *107*, 17–24. [CrossRef]
31. Ahmad, M.H.; Nache, M.; Waffenschmidt, S.; Hitzmann, B. Characterization of farinographic kneading process for different types of wheat flours using fluorescence spectroscopy and chemometrics. *Food Control.* **2016**, *66*, 44–52. [CrossRef]
32. Ghaffar, S.H.; Fan, M.; Zhou, Y.; Abo Madyan, O. Detailed Analysis of Wheat Straw Node and Internode for Their Prospective Efficient Utilization. *J. Agric. Food Chem.* **2017**, *65*, 9069–9077. [CrossRef] [PubMed]
33. Ghaffar, S.H.; Fan, M. Differential behaviour of nodes and internodes of wheat straw with various pre-treatments. *Biomass Bioenergy* **2015**, *83*, 373–382. [CrossRef]
34. Kalpokaitė-Dičkuvienė, R.; Lukošiūtė, I.; Brinkienė, K.; Striūgas, N.; Baltušnikas, A.; Lukauskaitė, R.; Čėsnienė, J. Utilization of sewage sludge-biomass gasification residue in cement-based materials: Effect of pozzolant type. *Environ. Technol.* **2017**, *39*, 2937–2950. [CrossRef] [PubMed]
35. Kalpokaitė-Dičkuvienė, R.; Baltušnikas, A.; Levinskas, R.; Čėsnienė, J. Incinerator residual ash—Metakaolin blended cements: Effect on cement hydration and properties. *Constr. Build. Mater.* **2019**, *206*, 297–306. [CrossRef]
36. Kalpokaitė-Dičkuvienė, R.; Lukošiūtė, S.I.; Baltušnikas, A.; Čėsnienė, J. Structural observation of cement paste modified with hydrophobic organoclay. *Constr. Build. Mater.* **2020**, *272*, 121931. [CrossRef]
37. Thommes, M.; Cychosz, K.A. Physical adsorption characterization of nanoporous materials: Progress and challenges. *Adsorption* **2014**, *20*, 233–250. [CrossRef]
38. Zhang, L.; Larsson, A.; Moldin, A.; Edlund, U. Comparison of lignin distribution, structure, and morphology in wheat straw and wood. *Ind. Crops Prod.* **2022**, *187*, 115432. [CrossRef]
39. Wang, Y.; Ji, X.-X.; Liu, S.; Tian, Z.; Si, C.; Wang, R.; Yang, G.; Wang, D. Effects of two different enzyme treatments on the microstructure of outer surface of wheat straw. *Adv. Compos. Hybrid Mater.* **2022**, *5*, 934–947. [CrossRef]
40. Nath, B.; Chen, G.; Bowtell, L.; Graham, E. Kinetic mechanism of wheat straw pellets combustion process with a thermogravimetric analyser. *Heliyon* **2023**, *9*, e20602. [CrossRef]
41. Sun, F.F.; Wang, L.; Hong, J.; Ren, J.; Du, F.; Hu, J.; Zhang, Z.; Zhou, B. The impact of glycerol organosolv pretreatment on the chemistry and enzymatic hydrolyzability of wheat straw. *Bioresour. Technol.* **2015**, *187*, 354–361. [CrossRef]
42. Shang, L.; Ahrenfeldt, J.; Holm, J.K.; Sanadi, A.R.; Barsberg, S.; Thomsen, T.; Stelte, W.; Henriksen, U.B. Changes of chemical and mechanical behavior of torrefied wheat straw. *Biomass Bioenergy* **2012**, *40*, 63–70. [CrossRef]

43. Shahryari, Z.; Fazaelipoor, M.H.; Setoodeh, P.; Nair, R.B.; Taherzadeh, M.J.; Ghasemi, Y. Utilization of wheat straw for fungal phytase production. *Int. J. Recycl. Org. Waste Agric.* **2018**, *7*, 345–355. [CrossRef]
44. Liu, X.-L.; Dong, C.; Leu, S.-Y.; Fang, Z.; Miao, Z.-D. Efficient saccharification of wheat straw pretreated by solid particle-assisted ball milling with waste washing liquor recycling. *Bioresour. Technol.* **2022**, *347*, 126721. [CrossRef] [PubMed]
45. Tessema, B.; Gonfa, G.; Hailegiorgis, S.M.; Sundramurthy, V.P. Characterization of teff straw from selected teff varieties from Ethiopia. *Heliyon* **2023**, *9*, e17422. [CrossRef] [PubMed]
46. Khorasani, M.; Naeimi, H. Fabrication and characterization of mesoporous yolk–shell nanocomposites as an effective reusable heterogeneous base catalyst for the synthesis of ortho-aminocarbonitrile tetrahydronaphthalenes. *RSC Adv.* **2023**, *13*, 18690–18699. [CrossRef] [PubMed]
47. Zaharescu, M.; Jitianu, A.; Brăileanu, A.; Madarász, J.; Novák, C.; Pokol, G. Composition and thermal stability of SiO_2-based hybrid materials TEOS-MTEOS system. *J. Therm. Anal. Calorim.* **2003**, *71*, 421–428. [CrossRef]